X-Ray characterization of self-assembled long-chain phosphatidylcholine/bile salt/silica mesostructured films with nanoscale homogeneity†

Darren R. Dunphy,[a] Fred L. Garcia,[a] Zhang Jiang,[b] Joseph Strzalka,[b] Jin Wang[b] and C. Jeffrey Brinker*[ac]

Received 17th September 2010, Accepted 18th November 2010
DOI: 10.1039/c0cc03919e

A bile salt (sodium taurodeoxycholate, NaTDC) was used to prevent phase separation between silica and lipid in self-assembled long-chain diacyl phosphatidylcholine/SiO_2 films. Phase diagrams for NaTDC/didecanoyl phosphatidylcholine/SiO_2 and NaTDC/egg phosphatidylcholine/SiO_2 films were investigated through grazing-incidence small-angle X-ray scattering at a synchrotron source.

The development of Cell-Directed Assembly (CDA)[1–4] and Cell-Directed Integration,[5] wherein living cells actively influence the bulk nanostructure of silica films templated by biocompatible short-chain or single-chain phosphatidylcholines[6] (PCs) during or after Evaporation-Induced Self-Assembly (EISA),[7] has created a new class of nano-bio interface that exhibits improved cell encapsulation properties over conventional sol–gel media[1,4,5] for applications including studies of cell confinement[2] and whole-cell biosensing. A fundamental restriction of the lipid/silica material composition used in CDA and CDI, however, is the necessity of using a diacyl PC with a tail length of less than 10 carbons or a lysoPC with only one acyl chain as the structure-directing agent to prevent total phase separation between silica and lipid during film assembly.[6] Incorporation of lipids with more biological relevance (*e.g.* diacyl PCs with tail lengths between 16 and 20 carbons) would facilitate the introduction of new behaviors for living cells encapsulated within these lipid/silica composites as well as permit the synthesis of new types of hybrid inorganic/biological nanocomposites.

To this end, we hypothesized that partition of a second, solubilizing lipid component into the PC phase would suppress this phase separation and facilitate the self-assembly of homogeneous lipid/silica mesophases for otherwise immiscible lipids. As a test of this strategy, we selected bile salts as the secondary lipid component, given the known ability of these lipids to solubilize lipid micelles and form mixed phases with PCs, including cubic phases with 3D lipid network connectivity.[8] Additionally, bile salts by themselves can organize into extended liquid crystalline mesophases in water,[9] possibly creating lipid/silica materials with improved material properties when compared with films using PCs as the lipid component (*i.e.* stability of the pore volume after lipid removal).

For a bile salt, sodium taurodeoxycholate (NaTDC, structure given in Fig. 1A) was selected as the co-lipid based on compatibility with the low-pH sol–gel chemistry generally used in EISA. The first test of using a secondary lipid to prevent phase separation was performed using didecanoyl PC ($di C_{10}PC$), a lipid previously found to completely phase separate from silica during film assembly (Fig. 2A).[6] Grazing-incidence small-angle X-ray scattering (GISAXS), performed at beamline 8ID at the Advance Photon Source, Argonne National Laboratories, was used to confirm the formation of non-phase separated nanostructured lipid/silica mesophases, and to identify the specific type of phases present in these hybrid materials. In GISAXS, an X-ray beam is incident onto a supported thin film at an angle greater than the critical angle of the film, but less than the critical angle of the substrate, maximizing the interaction volume between beam and nanostructured material, enabling the structural investigation of nanostructured films as thin as one monolayer over large-scale

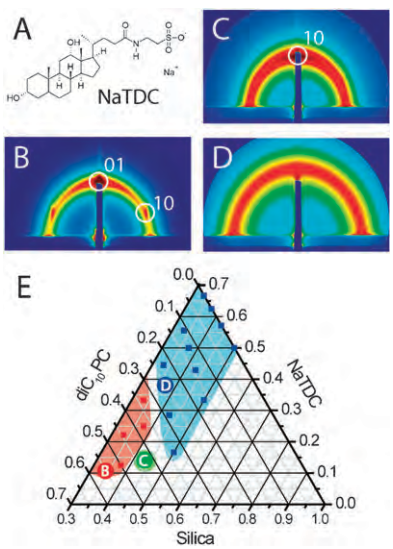

Fig. 1 (A) Structure of the bile salt sodium taurodeoxycholate (NaTDC), (B–D) GISAXS data for mesophases formed from a mixture of $di C_{10}PC$ and NaTDC in silica using an EISA process; (B) 2D hexagonal phase, (C) oriented lamellar phase, (D) disordered phase, (E) ternary phase diagram obtained using GISAXS data between silica, NaTDC, and $di C_{10}PC$, with locations of GISAXS data points from panels (B–D) labelled in circles. Red signifies regions of hexagonal order, with green and blue indicating lamellar and disordered packing, respectively.

[a] *The University of New Mexico/NSF Center for Micro-Engineered Materials, Chemical and Nuclear Engineering Department, Albuquerque, New Mexico, 87131b, USA*
[b] *Argonne National Laboratory Advanced Photon Source, Argonne, IL 60439, USA*
[c] *Sandia National laboratories, Advanced Materials Lab, 1001 University Blvd. SE, Albuquerque, New Mexico, 87106, USA. E-mail: cjbrink@sandia.gov; Fax: 505-272-7336; Tel: 505-272-7627*

† Electronic supplementary information (ESI) available: Details of film synthesis; cell-directed assembly. See DOI: 10.1039/c0cc03919e

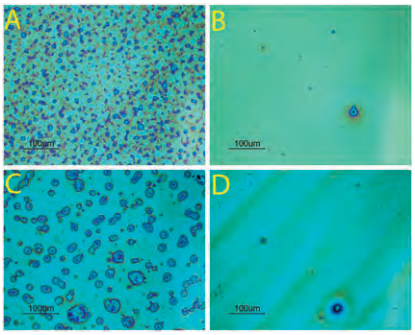

Fig. 2 (A) Optical micrograph of *di*C_{10}PC/silica film, showing complete phase separation between lipid and silica. (B) Typical NaTDC/*di*C_{10}PC/silica film (NaTDC/*di*C_{10}PC mass ratio = 1) demonstrating formation of a macroscopically homogenous nanostructure. (C) NaTDC/egg PC/silica film containing regions of partial phase separation between nanostructured lipid/silica and silica. (D) As (C), but with decreased total lipid/silica ratio. Film features are artifacts of the spin coating process.

areas.[10] A wide composition range in the *di*C_{10}PC/NaTDC/silica system was examined, with typical GISAXS data shown in Fig. 1B–D along with the phase diagram determined using this data in Fig. 1E. For this phase diagram, plotted in units of volume percentage, the density of both *di*C_{10}PC and NaTDC was assumed to be 1.0 g cm^{-3}, with the density of the amorphous silica framework estimated to be 2.2 g cm^{-3}. Importantly, in all film compositions studied within this phase diagram, there was no evidence of phase separation as seen by optical microscopy, indicating the formation of macroscopically homogeneous lipid/silica mesophases (Fig. 2B). Nanoscale phase separation between lipids was also not observed, as demonstrated by the presence of scattering from only one nanostructure within all GISAXS images.

Without NaTDC, *di*C_{10}PC phase separates into a lamellar phase with an interlayer spacing of 34 Å.[6] With NaTDC, three distinct phase regions were observed. At high *di*C_{10}PC volume fractions, a 2D hexagonal phase of cylindrical lipid micelles within a silica framework, packed parallel to the substrate, is found (Fig. 1B); as evidenced by the presence of an isotropic ring within the GISAXS data connecting the {01} diffraction spots, this phase has imperfect alignment with respect to the surface, with the degree of orientational order further reduced as the volume fraction of *di*C_{10}PC is decreased. Lattice parameters for this hexagonal packing range from a = 47.6 Å to a = 40.0 Å in the plane of the substrate, with drying stresses perpendicular to the film thickness inducing condensation of silica and yielding a *ca.* 20% shrinkage in lattice parameters. Phases of pure lipid (without silica) do not exhibit this anisotropic shrinkage, supporting the presence of a mixed lipid/silica phase. A lamellar phase comprised of alternating layers of lipid and silica, again with imperfect orientation relative to the substrate as shown by the presence of an isotropic ring in the GISAXS data, occurs at a lower total lipid/silica ratio (Fig. 1C). Comparison of the lattice parameters for this phase parallel to the substrate (50.5 Å) with that normal to the substrate (39.4 Å) again shows a 20% uniaxial compression from the presence of silica within the nanostructure. At high NaTDC/*di*C_{10}PC ratios, isotropic diffraction rings indicate the lack of any preferential orientation for film nanostructure; it is not possible to distinguish between non-oriented lamellar, non-oriented hexagonal, and disordered micellular phases from the isotropic scattering rings observed for compositions prepared in the blue area in Fig. 1E. The correlation length of this non-oriented nanostructure ranges from 55 Å for a *di*C_{10}PC/NaTDC volume ratio of *ca.* 2 to 33–38 Å for NaTDC alone, with no evidence of 2D hexagonal packing for this bile salt as seen in the NaTDC/H_2O phase diagram.[9]

Removal of the lipid phase in these *di*C_{10}PC/NaTDC/silica composites by UV/O_3[11] or thermal degradation results in collapse of porosity templated by the lipid mesophase, a behavior identical to that seen in silica containing short-chain PCs[6] where, relative to other common EISA templates (*e.g.*, cetyltrimethylammonium bromide), FTIR, NMR, and X-ray studies[6] have shown inhibited condensation of framework silica due to strong interactions with lipid headgroups. Porosity in silica films templated by NaTDC alone was also unstable toward lipid removal; whether this is also an effect of headgroup interactions or geometric pore instability is presently unknown. Replacement of the silica precursor with a hybrid organic/inorganic sol–gel precursor (bis(triethoxysilyl)ethane, BTESE) was previously found to produce stable porosity in PC-templated films, with mesophase type identical to the corresponding silica films;[6] here, however, *di*C_{10}PC/NaTDC/BTESE and NaTDC/BTESE films were found to be less ordered than the silica materials, with collapse of the mesostructure parallel to the substrate during calcination indicating formation of non-oriented lamellar phases.

Bile salts solubilize PC lamellar phases through an increase of head group area as well as through the introduction of electrostatic forces between and within lamellae;[8] we posit a similar mechanism reduces aggregation of PC during the EISA process. Modulation of lipid–silica interactions by introduction of the bile salt is not likely to be a significant factor in the prevention of phase separation; previous work has already shown a strong intermixing between between PC headgroup and silica, with phase separation being driven by the rapid reduction of lipid critical micelle concentration as the tail length increases.[6] Furthermore, electrostatic interactions are purposely suppressed in EISA by selection of sol pH to match the isoelectric point of silica (*ca.* pH 2).

A lipid mixture with more biological relevance is that of egg PC, a lipid mixture with an approximate fatty acid composition of 16 : 0 (signifying a tail length of 16 carbons with zero unsaturated bonds, 32.7%), 18 : 1 (32%), 18 : 2 (17.1%), and 18 : 0 (12.3%). Like *di*C_{10}PC, without NaTDC there is complete phase separation between lipid and silica. With NaTDC, however, lamellar (Fig. 3A), 2D hexagonal (Fig. 3B), and disordered phases are present in the NaTDC/egg PC/silica phase diagram (Fig. 3D). Without silica, egg PC forms a lamellar phase with d = 40 Å. Layer spacing for the NaTDC/egg PC/silica lamellar phase ranges from 55 Å to 70 Å, while the lattice parameter a for the 2D hexagonal phases ranges from *ca.* 40–44 Å. Overall, the degree of orientation and nanostructure order in these phases is better than that for NaTDC/*di*C_{10}PC/silica films; as an example, Fig. 3B shows scattering for a 2D hexagonal phase with strong 2nd order diffraction peaks. Again,

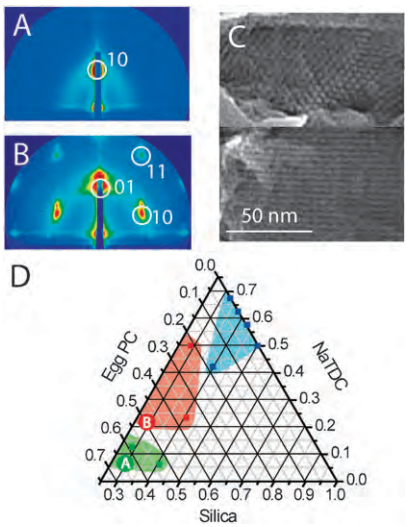

Fig. 3 (A–B) GISAXS data for mesophases formed from a mixture of egg PC and NaTDC in silica using an EISA process; (A) oriented lamellar phase, (B) 2D hexagonal phase. The double reflections are due to scattering from both the incident and reflected X-ray beam. (C) TEM images of the silica/egg PC/NaTDC phase from panel (B) (top is a cross-sectional view, in the direction of the cylindrical micelles, bottom is a plan-view normal to the plane of the substrate). These TEM images were obtained from the same film analyzed by GISAXS in panel (B). (D) ternary phase diagram obtained using GISAXS data between silica, NaTDC, and egg PC, with locations of GISAXS data points from panels (A) and (B) labelled in circles. Red signifies regions of hexagonal order, with green and blue indicating lamellar and disordered packing, respectively.

shrinkage of the nanostructure perpendicular to the film thickness of *ca.* 10–20% (as seen in Fig. 3A and B) supports the presence of silica within the lipid nanostructure.

Similar to the case of films made with *di*C_{10}PC, the NaTDC/egg PC/silica nanostructures were found to be unstable toward lipid removal. A key difference between the two systems, however, is that examination of NaTDC/egg PC/silica films with an optical microscope does reveal the presence of some phase separation (Fig. 2C). Yet, unlike the case of films synthesized without NaTDC, where phase separation produces waxy droplets of pure lipid within the silica film, this phase separation does not appear to be between silica and lipid, but rather between regions of lipid/silica composite and pure silica. The regions of apparent phase separation are resistant to mechanical abrasion, indicating the presence of a silica framework within these areas of the film. Also, TEM analysis of a film with 2D hexagonal structure shows regions of silica film without any lipid present along with nanostructured areas consistent with the presence of a lipid/silica mesophase (Fig. 3C); energy dispersive X-ray spectroscopy (EDS) shows both lipid and silica within the nanostructure, with the stability of the observed nanostructure under the electron beam irradiation being further evidence that a lipid/silica mesophase is present. By decreasing the volume percentage of silica in the nanocomposite film but keeping the NaTDC to egg PC ratio constant, or by increasing the NaTDC to egg PC ratio at a given volume percentage of silica, we find that this partial phase separation is eliminated (Fig. 2D). Also, reduction of sol aging time or increased spin coating speed were found to reduce the degree of phase separation, suggesting that control of lipid–silica interactions as well as self-assembly kinetics may be used to minimize this effect.

In summary, we have demonstrated a strategy for the synthesis of PC/silica nanostructured films using lipids that normally phase separate during film assembly, incorporating a bile salt as a co-lipid to reduce PC aggregation. Preliminary experiments show the feasibility of using long-chain lipid/NaTDC compositions in CDA (see ESI†); future work will refine these results, as well as examine the fabrication of new functional lipid/silica nanostructures (for example, homogeneously incorporating transmembrane proteins within an oriented lipid mesophase network).[12]

Use of the APS is supported by the Department of Energy under contract DE-AC02-06CH11357. Sandia is a multi-program laboratory operated by Sandia Corporation, a Lockheed Martin Company, for the United States Department of Energy's National Nuclear Security Administration under contract DE-AC04-94AL85000. Eric Carnes and Robert Castillo are thanked for their assistance with CDA.

Notes and references

1 H. K. Baca, C. Ashley, E. Carnes, D. Lopez, J. Flemming, D. Dunphy, S. Singh, Z. Chen, N. Liu, H. Fan, G. P. Lopez, S. M. Brozik, M. Werner-Washburne and C. J. Brinker, *Science*, 2006, **31**, 337.
2 E. Carnes, D. Lopez, H. Gresham, A. Cheung, G. Timmins and C. Brinker, *Nat. Chem. Biol.*, 2009, **6**, 41.
3 E. C. Carnes, J. C. Harper, C. E. Ashley, D. M. Lopez, L. M. Brinker, J. W. Liu, S. Singh, S. M. Brozik and C. J. Brinker, *J. Am. Chem. Soc.*, 2009, **131**, 14255.
4 H. K. Baca, E. Carnes, S. Singh, C. Ashley, D. Lopez and C. J. Brinker, *Acc. Chem. Res.*, 2007, **40**, 836.
5 J. C. Harper, C. Y. Khirpin, E. C. Carnes, C. E. Ashley, D. M. Lopez, T. Savage, H. D. T. Jones, R. W. Davis, D. E. Nunez, L. M. Brinker, B. Kaehr, S. M. Brozik and C. J. Brinker, *ACS Nano*, **4**, 5539.
6 D. R. Dunphy, T. M. Alam, M. P. Tate, H. W. Hillhouse, B. Smarsly, A. D. Collord, E. Carnes, H. K. Baca, R. Kohn, M. Sprung, J. Wang and C. J. Brinker, *Langmuir*, 2009, **25**, 9500.
7 Y. F. Lu, R. Ganguli, C. A. Drewien, M. T. Anderson, C. J. Brinker, W. L. Gong, Y. X. Guo, H. Soyez, B. Dunn, M. H. Huang and J. I. Zink, *Nature*, 1997, **389**, 364.
8 J. Ulmius, G. Lindblom, H. Wennerstroem, L. B. A. Johansson, K. Fontell, O. Soederman and G. Arvidson, *Biochemistry*, 2002, **21**, 1553.
9 E. F. Marques, H. Edlund, C. La Mesa and A. Khan, *Langmuir*, 2000, **16**, 5178.
10 J. Pang, S. Xiong, F. Jaeckel, Z. Sun, D. Dunphy and C. Brinker, *J. Am. Chem. Soc.*, 2008, **130**, 3284.
11 T. Clark, R. D. Ruiz, H. Fan, C. J. Brinker, B. I. Swanson and A. N. Parikh, *Chem. Mater.*, 2000, **12**, 3879.
12 S. A. Yamanaka, D. H. Charych, D. A. Loy and D. Y. Sasaki, *Langmuir*, 1997, **13**, 5049.

